Polymer 50 (2009) 2674–2679

Contents lists available at ScienceDirect

Polymer

journal homepage: www.elsevier.com/locate/polymer

Conducting polyaniline film from aqueous dispersion: Crystallizable side chain forced lamellar structure for high conductivity

Hongming Zhang, Xianhong Wang*, Ji Li, Zhishen Mo, Fosong Wang

State Key Lab of Polymer Physics and Chemistry, Changchun Institute of Applied Chemistry, CAS, Changchun 130022, PR China

ARTICLE INFO

Article history:
Received 19 December 2008
Received in revised form
3 April 2009
Accepted 14 April 2009
Available online 21 April 2009

Keywords:
Polyaniline
Aqueous dispersion
High conductivity

ABSTRACT

Aqueous conducting polyaniline dispersion was prepared employing acidic phosphate ester bearing hydrophilic ethylene glycol segment as dopant, and conducting film with electrical conductivity of 25 S/cm was obtained from the dispersion. Ordered self-assembly lamellar structure with interlamellar distance of 1.2 nm was observed in the film, which consisted of alternating layers of rigid polyaniline chain and flexible phosphate ester side chains, where the phosphate side chain layer was separated by two rigid polyaniline layers. The lamellar structure leading to high conducting film was formed due to the confinement of polyaniline chain by crystallizable phosphate side chain, since the electrical conductivity decreased by four orders of magnitude once the dopant side chain crystalline was destroyed. The crystallizable side chain forced lamellar structure is expected to be a new chance for highly conducting polyaniline.

1. Introduction

With the increasing environmental concern [1,2], water-borne conducting polyaniline has been prepared by various approaches, such as self-doped polyaniline [3], colloidal dispersion [4] and counter-ion induced processability [5]. However, the low electrical conductivity (e.g., 10^{-9} S/cm to 10^{-1} S/cm) [6] of the casting film was far from satisfactory. Earlier work by this group succeeded in preparing water-soluble conducting polyaniline (cPANI), employing acidic phosphate ester with relatively longer hydrophilic ethylene glycol segment as dopant, again giving electrical conductivity of below 10^{-1} S/cm [7]. Recently, we proposed an aqueous dispersion route, employing a short segment phosphate ester as dopant for polyaniline emeraldine base (PANI-EB), and a conductivity of 4–5 S/cm was easily achieved [8]. An unpublished work in this lab showed that the electrical conductivity could even reach as high as 25 S/cm, not only much higher than those of earlier reported water-borne polyaniline [2,3,6], but also one order of magnitude higher than that of hydrochloric acid doped polyaniline [9].

The structure of conducting polyaniline was of key importance for electrical conductivity [10–16], a typical example was camphor sulfonic acid doped polyaniline whose electrical conductivity reached 300 S/cm from *m*-cresol solution [10,14,15]. Dodecylbenzenesulfonic acid was another effective dopant of polyaniline producing honeycomb self-assembly structure [17] with electrical conductivity of 3.5 S/cm, in addition, orthorhombic crystalline [18] and lamellar structure [19] was also found. Dialkyl or dialkoxy esters of sulfoisophthalic acid, sulfophthalic acid or sulfosuccinic acid can also facilitate the lamellar self-assembly, and high electrical conductivity up to ca. 200 S/cm was realized from dichloroacetic acid solution [20–22]. Cylindrical self-assembly structure has been obtained using 2-acrylamido-2-methyl-1-propanesulfonic acid and its conductivity increased up to 4 orders of magnitude from 10^{-4} S/cm to 6 S/cm [23]. The high conductivities were explained based on crystallization structures [15] and molecularly matching bonds formed among polyaniline, dopant and solvent such as phenols and 4-hexylresorcinol [18]. Though the above investigations were carried out in organic cPANI system, the correlation between structure and conductivity for cPANI must be beneficial for water-borne system.

In this paper, aqueous conducting polyaniline film was prepared with electrical conductivity of 25 S/cm. Aiming to disclose a feasible route to prepare high electrical conducting polyaniline film from aqueous dispersion, the relationship between structure and conductivity was investigated by UV–vis spectroscopy, X-ray photoelectron spectroscopy (XPS), transmission electron microscope (TEM) and wide-angle X-ray diffraction (WAXD) techniques.

2. Experimental section

2.1. Materials

Various ethylene glycol monomethyl ethers (EGMEs) with different repeating units of ethylene glycol segment were provided

---

* Corresponding author. Tel.: +86 431 85262250; fax: +86 431 85689095.
E-mail address: xhwang@ciac.jl.cn (X. Wang).

0032-3861/$ – see front matter © 2009 Elsevier Ltd. All rights reserved.
doi:10.1016/j.polymer.2009.04.020

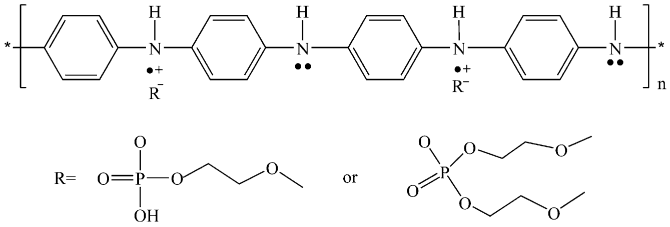

Scheme 1. Simplified structure of aqueous dispersed polyaniline.

by Aldrich. PANI-EB is the product of Benan Co. (China) licensed under this lab, and its intrinsic viscosity of 0.1 wt% in *N*-methyl-2-pyrrolidone is 4.0 mPa s at 25 °C.

2.2. Preparation of acidic phosphate ester dopant

The typical procedure was shown as follows [24]: 25.6 g (0.18 mol) of phosphorus pentoxide was added to 22.8 g (0.3 mol) of EGME ($M_n = 76$) in 50 mL tetrachloride carbon and then the mixture was heated to 65 °C and stirred for 8 h. After the mixture was stirred for 24 h, 12 mL of distilled water was added, and the mixture was kept stirring for 2 h. The reaction mixture was decolored by activated carbon to give a pale yellow transparent acidic phosphate ester. The total acid value of the phosphate ester was 5.68 mmol/g determined by potentiometric titration with an ORION model 710A PH/ISE meter using predetermined sodium hydroxide solution. The molar ratio of monoester to diester was 3.2:1, and the side chain of the phosphate ester was composed of one unit of hydrophilic ethylene glycol which was shorter than that in our recent report [8].

2.3. Preparation of phosphate ester doped PANI-EB aqueous dispersion

Aqueous dispersion was prepared by dispersing the acidic phosphate ester into PANI-EB powder in distilled water [8]. The procedure was carried out as follows: the phosphate ester doped PANI-EB was obtained by adding 1.06 g emeraldine base and 2.13 g phosphate ester into 50 mL distilled water with stirring for 72 h at 60 °C. The simplified structure of the conducting polyaniline is shown in Scheme 1, in which the acidic phosphate ester radical cation [25] is linked with polyaniline chain.

In another aspect, the aqueous cPANI solution was prepared according to the similar approach as the synthesis of above aqueous polyaniline dispersion, and it was used as a reference. Compared with the structure of aqueous dispersion, the acidic phosphate ester radical cation charge consisted of 7 units of ethylene glycol segment (Scheme 2) [2,3,6] which was longer than that of aqueous dispersed polyaniline.

2.4. Measurements

UV–vis spectra of acidic phosphate ester doped PANI-EB aqueous dispersion were recorded at room temperature using a Lambda 900 spectrophotometer (Perkin Elmer) in the wavelength range 300–1400 nm. The diameter of cPANI particle was determined by dynamic light scattering (DLS) at 25 °C with a vertically polarized He–Ne laser (DAWN EOS, Wyatt Technology, laser wavelength of 690 nm). XPS measurements were carried out on a VG ESCALAB MkII spectrometer with a Mg Ka X-ray source (1253.6 eV photos), where the X-ray source was operated at 14 kV and 20 mA, and the sample was mounted onto standard VG sample stud with double-sided adhesive tape. The pressure in the XPS analysis chamber was maintained at 10^{-7} Pa or lower during data collection. The sample position and tilt angle were finely tuned for optimal data acquisition. The C 1s neutral carbon peak at 284.6 eV was used as the reference for all binding energies (BEs). The core-level spectrum was deconvoluted into Gaussian component peaks. Wide-angle X-ray

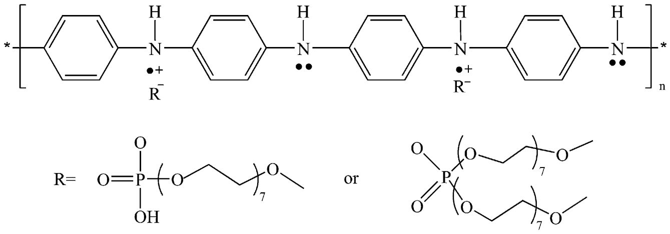

Scheme 2. Simplified structure of water-soluble polyaniline.

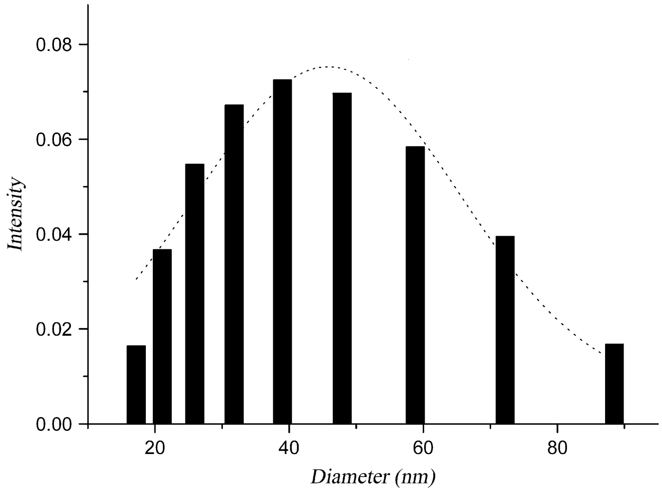

Fig. 1. DLS spectrum of the aqueous dispersion.

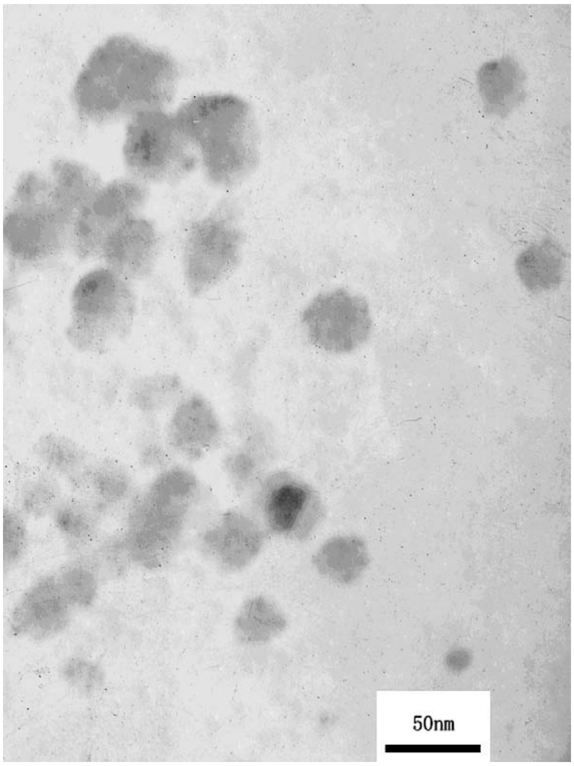

Fig. 2. TEM image of the aqueous dispersion.

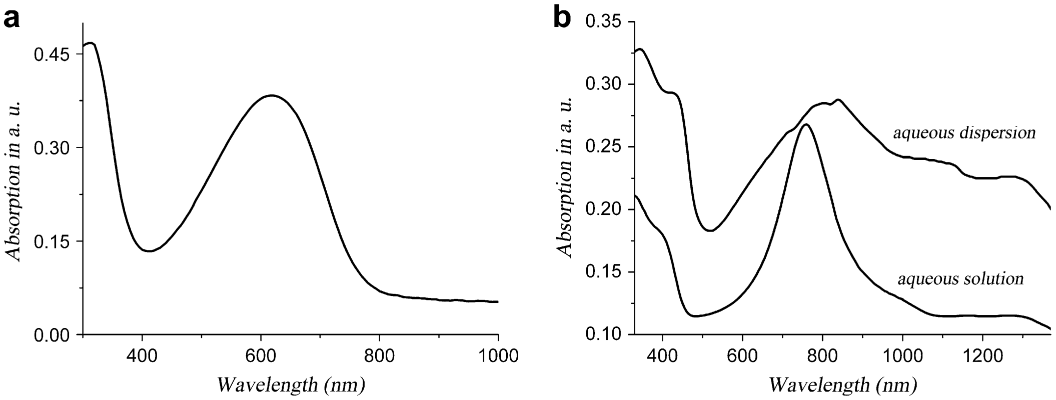

Fig. 3. UV–vis absorption spectra of EB in *N*-methyl-2-pyrrolidone (a), aqueous cPANI solution (electrical conductivity: 0.1 S/cm) and aqueous cPANI dispersion (electrical conductivity: 25 S/cm) (b).

diffraction (WAXD) patterns were recorded using Cu Kα ($\lambda = 1.5406$ Å) radiation at 40 kV and 40 mA with PW1700 X. X-ray diffractometer scanned between angle 2θ of 5–35° in a step size of 0.1°/s and scan rate of 1°/min. TEM image was obtained on a JEOL JEM-2010 transmission electron microscope at an acceleration voltage of 200 kV. Samples for TEM were prepared by drop casting of diluted aqueous dispersion on carbon-coated copper grids and allowing them to dry freely. Casting films were dried in vacuum at 25 °C for 5 days before electrical conductivity measurement according to standard four-probe method. As for the electrical conductivity, WAXD and UV–vis of cPANI films' dependence on temperatures, the films were controlled for 30 min at different temperatures ranging from 25 °C to 200 °C. After cooling to room temperature the corresponding measurements were carried out.

3. Results and discussion

According to DLS spectrum shown in Fig. 1, the spherical particles had a mean diameter around 48 nm, where about 92% of the particles ranged between 20 and 80 nm. To confirm particle morphology, the TEM studies of aqueous dispersion are shown in Fig. 2. This result indicated that the doping of PANI-EB produced spherical particles with size range 20–80 nm, where the nanosize was quite comparable with the DLS results.

The aqueous dispersion was dark-green in color, it was very stable in that no precipitation was observed even after six months, and the particle size distribution was almost unchanged for one year.

The UV–vis spectra of EB in *N*-methyl-2-pyrrolidone solution and aqueous cPANI dispersion are shown in Fig. 3, the aqueous cPANI solution with electrical conductivity of ca. 10^{-1} S/cm [7] is also listed as a comparison. Strong absorption peaks at 315 nm and 620 nm were observed in EB solution, characteristic of π–π^* transition of the benzenoid structure and exciton transition of the quinoid structure [26]. For aqueous polyaniline solution, absorption peaks at 403 nm and 760 nm characteristic of polaron bands indicated that polyaniline was in doped state [27], but the strong absorption peak at 760 nm indicated that the carrier species were mainly the localized radical cations, or a compact coil-like conformation of polyaniline chain, leading to relatively low electrical conductivity [28]. As for the aqueous cPANI dispersion, the absorption peak at 315 nm in EB red-shifted to 350 nm, the peak at 620 nm in EB disappeared, and a shoulder absorption peak at 435 nm from semiquinoid radical cation appeared [29], moreover, a broad cationic radical polaron band appeared starting from 830 nm to 1330 nm. The new broad absorption peak at above 1000 nm may be attributed to the free carrier tail [30], indicating more delocalized carrier species, or a more extended conformation of the conducting polyaniline chains, leading to significant electrical conductivity increase by at least two orders of magnitude.

The change of oxidation state in EB and cPANI film cast from aqueous dispersion was investigated by XPS technique [31]. As shown in Fig. 4, the symmetric N 1s spectrum of EB can be deconvoluted into two peaks, one at 398.4 eV was assigned to quinoid imine (=N–) with a full width at half-maximum (FWHM) of 1.07 eV, and the other at 399.5 eV was attributed to benzenoid

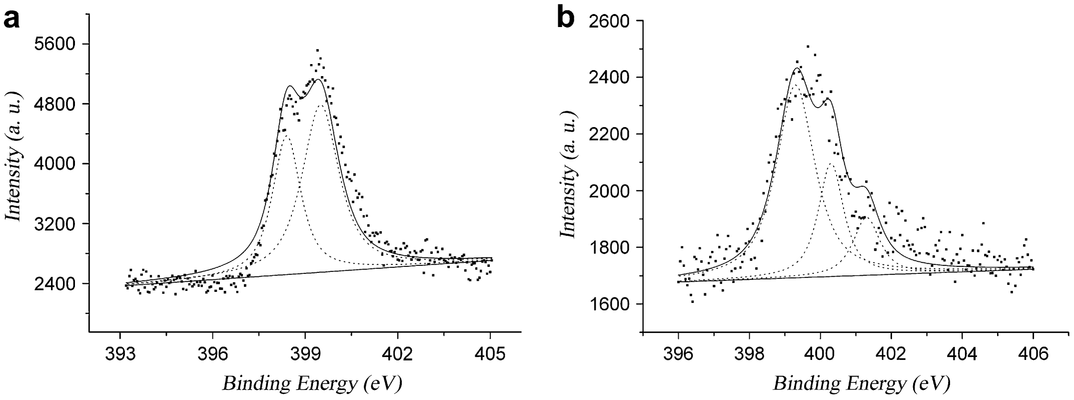

Fig. 4. N 1s XPS core-level spectra of EB film (a) and cPANI film from aqueous dispersion (b).

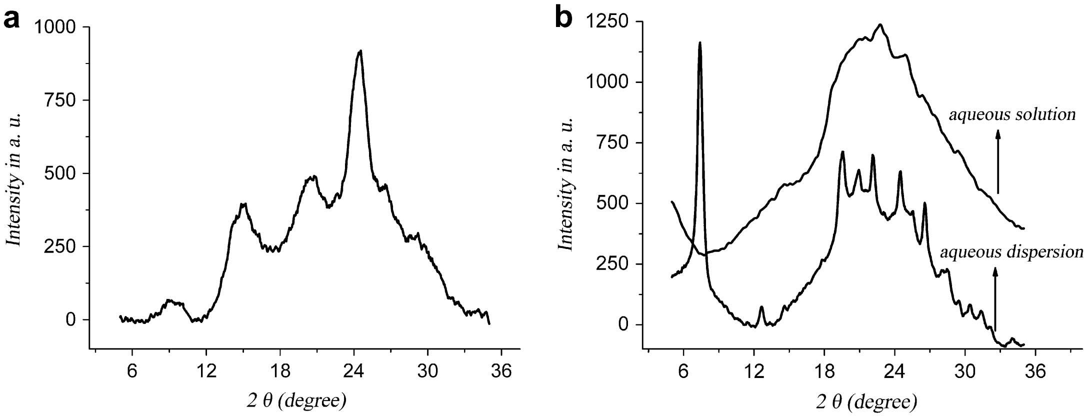

Fig. 5. WAXD of EB powder (a), cPANI film cast from aqueous dispersion or solution (b).

amine (–N–) with an FWHM of 1.37 eV. The asymmetric N 1s core level of cPANI from aqueous dispersion was deconvoluted into three peaks, one centered at 400.3 eV with an FWHM of 0.84 eV from the radical cation nitrogen atoms with delocalized positive charge, the second one located at 401.4 eV with an FWHM of 0.88 eV from iminium ions (–NH$^+$=) [32], and the third one at 399.4 eV with an FWHM of 1.22 eV from benzenediamine (–N–). Since the quinonediimine (=N–) peak at 398.4 eV vanished completely, while the peak characteristic of radical cation appeared, indicating that all the imine nitrogen atoms were converted into the positively charged nitrogen species, which was consistent with the existence of semiquinoid radical cation in UV spectra. In another aspect, the area fraction of these three peaks was 0.25, 0.15 and 0.60, respectively, where the positively charged nitrogen atoms were 40% of the total area, implying that the doping level of aqueous dispersion was 40%, which was higher

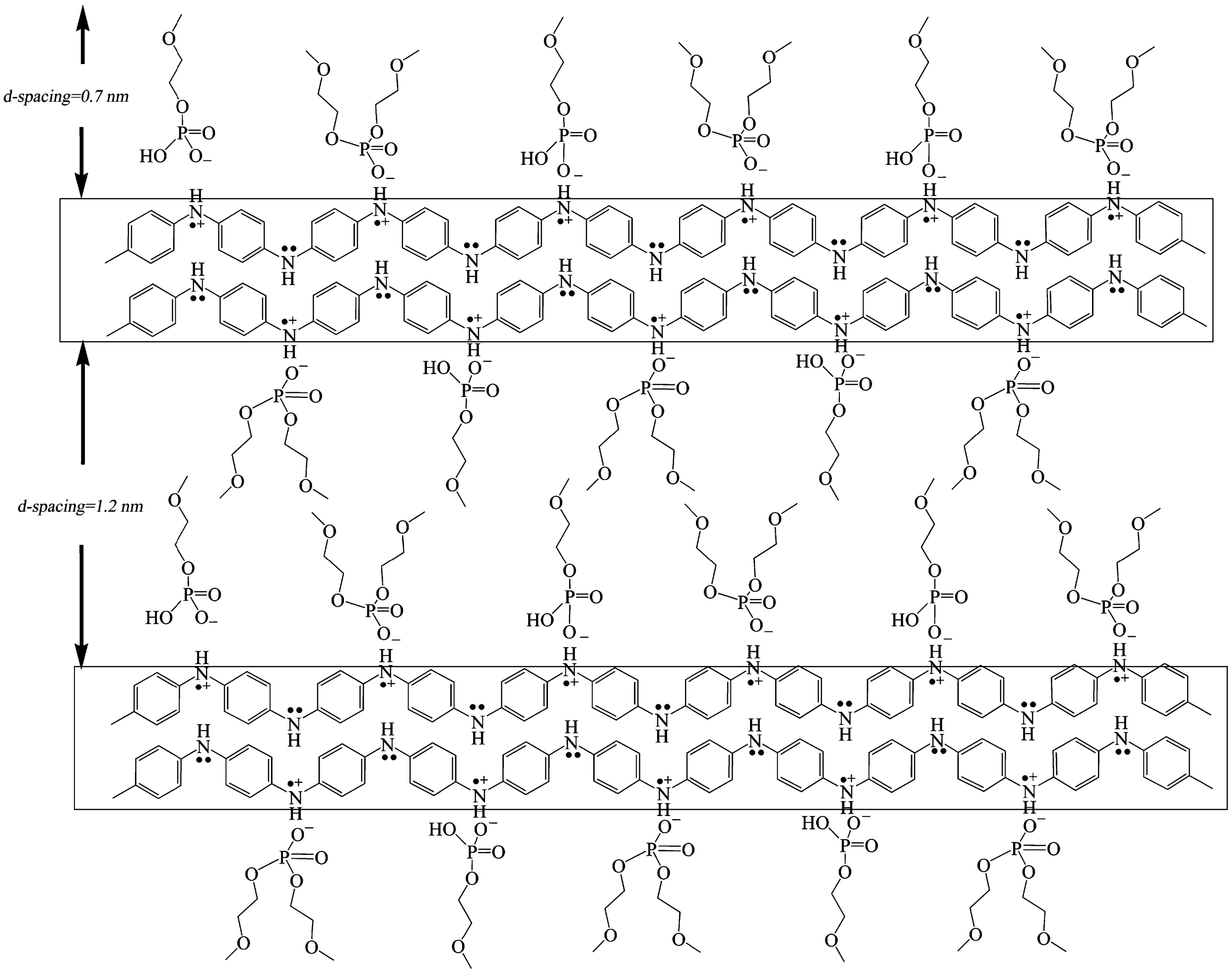

Fig. 6. Schematic illustration of the lamellar structure consisting of alternating polyaniline layer and phosphate ester side chain layer.

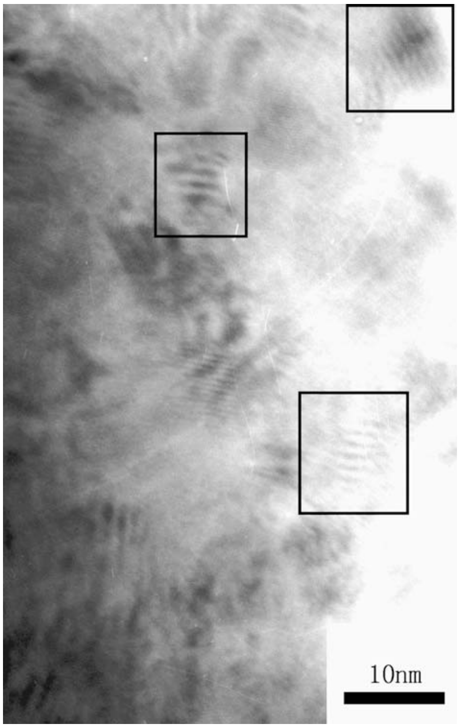

Fig. 7. TEM micrograph of aqueous cPANI dispersion for stripe.

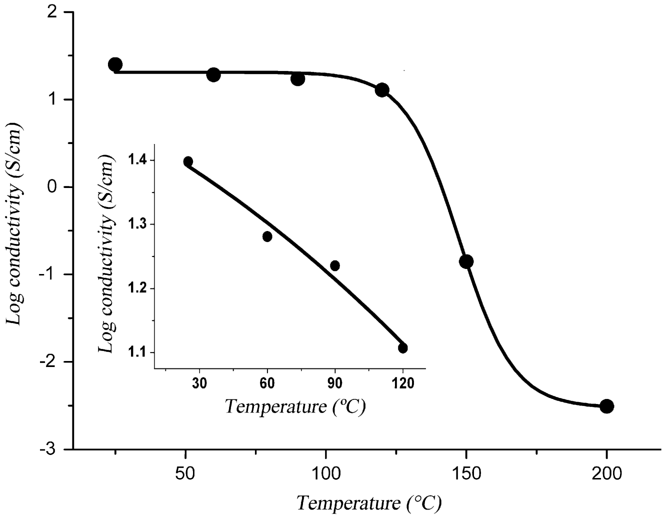

Fig. 9. Electrical conductivity of cPANI film from aqueous dispersion at different temperatures, inset shows the dependence of conductivity on temperature from 25 °C to 120 °C.

than water-soluble self-doped conducting polyaniline [33], providing good support for its high electrical conductivity.

The crystalline structure of cPANI from aqueous dispersion was studied by WAXD. As shown in Fig. 5a, the WAXD pattern of EB powder exhibits a broad reflection centered at $2\theta = 20.4°$ and a large FWHM of 8° at $2\theta = 24.4°$, indicating that EB was partly crystalline [34–36]. However, no pronounced diffraction peak was observed in the WAXD pattern of cPANI film from aqueous solution (Fig. 5b), indicating that no crystalline structure existed in this film, since the ordered packing of the doped chains was inhibited by the conformational hindrance as well as the large size of the side chain in dopant [29]. The WAXD pattern of cPANI film cast from aqueous dispersion showed several diffraction peaks (Fig. 5b), indicating that ordered structure existed in the film. It should be noted that the phosphate ester dopant was in amorphous liquid state at room temperature, and hence the diffraction peaks were due to the doped polyaniline. The peak at $2\theta = 24.5°$ may be due to the periodicity perpendicular to the polyaniline chain [37], and the peaks such as $2\theta = 14.6°$, 20.9°, 22.1°, 25.5°, 26.6°, 28.5°, 30.5° and 31.4° may be caused by the branches of dopant interacting with polyaniline chain at various directions [38]. A novel diffraction peak at low angle of $2\theta = 7.45°$ with a small FWHM of 0.5° appeared in strong intensity, indicating the existence of crystallization and ordered arrangement for cPANI chain. Another new diffraction peak at $2\theta = 12.6°$ with an FWHM of 0.3° can be ascribed to the phosphate ester anion. According to GAUSSIAN 03 theoretical calculation, the theoretical dimension of phosphate ester side chains was 0.75 nm [39], since two *d*-spacings for dopant side chains of 0.70 nm ($2\theta = 12.6°$) and 1.2 nm ($2\theta = 7.45°$) were observed [34], it can be assumed that each flexible layer contained a bilayer of phosphate ester side chains with a limited interdigitation. In addition, according to GAUSSIAN 03 calculation, the theoretical length of benzene ring was 0.24 nm, the existing *d*-spacing of 0.46 nm ($2\theta = 19.6°$) in the WAXD pattern indicated that each rigid layer contained a bilayer of polyaniline chains. Therefore, a lamellar self-assembly structure is proposed and shown in Fig. 6, in which

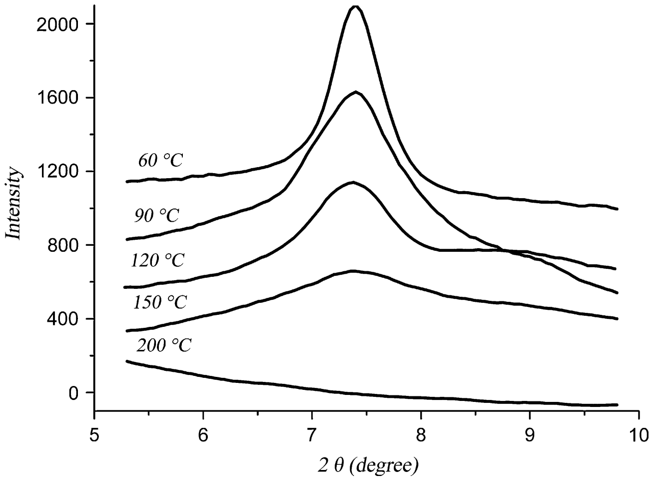

Fig. 8. WAXD curves of cPANI film cast from aqueous dispersion at different temperatures.

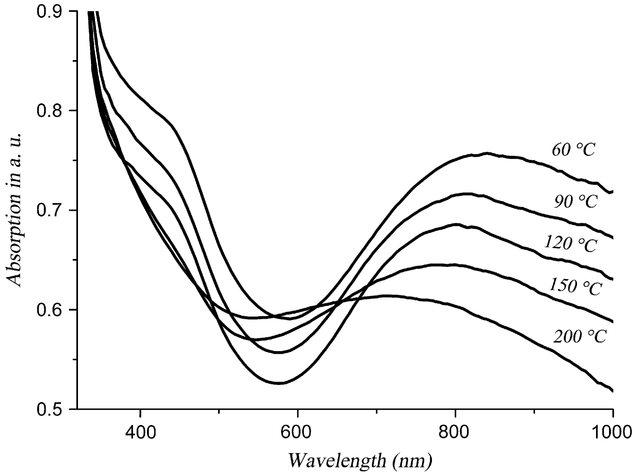

Fig. 10. UV–vis spectra for cPANI film cast from aqueous dispersion at various temperatures.

the lamellar structure consisted of alternating layers of polyaniline chain and flexible phosphate ester side chains, and the phosphate side chain layer is separated by two rigid polyaniline chain layers.

As indicated in rectangle area of the TEM images in Fig. 7, alternating bright and dark layers of uniform stripe thickness oriented in different direction were observed, and the thickness of the dark and the bright layers was ca. 1.2 nm, the nanoscale lamellar structure with the interlamellar distance was coincident with above Bragg distance d-spacing of 1.2 nm ($2\theta = 7.45^\circ$) obtained from WAXD pattern, indicating that self-assembly lamellar morphology was achieved at room temperature.

The Bragg distance d-spacing of 0.70 nm for $2\theta = 12.6^\circ$ and 1.2 nm for $2\theta = 7.45^\circ$ confirmed that phosphate ester side chain underwent crystallization, similar result was also reported in polyaniline doped by sulfonic ester containing long side chain [40]. To investigate the dependence of crystal structure on the conductivity, temperature factor was considered. As shown in Fig. 8, when the temperature increased from 60 °C to 200 °C, the intensity of WAXD peak decreased significantly and FWHM of this reflection was broadened, indicating the elimination of ordered structure in cPANI film, providing further evidence for the side chain crystallization in cPANI.

The dependence of electrical conductivity of cPANI film on temperature is depicted in Fig. 9. The conductivity decreased slowly with increasing temperature from room temperature to 120 °C, and it dropped rapidly above 120 °C, nearly four orders of magnitude reduction at 200 °C than that at room temperature, which was mainly due to the complete destruction of side chain crystalline structure.

The electronic structure change of cPANI film from aqueous dispersion is followed by UV–vis spectra at various temperatures in Fig. 10. When the temperature increased from 60 °C to 200 °C, a blue shift of 120 nm was observed. Polyaniline chains generally took a more extended and ordered structure at low temperature due to the confinement of the side chain crystalline, once the crystalline structure was destroyed at higher temperature, the confinement force disappeared, and disordered chains became dominant.

4. Conclusions

Aqueous cPANI dispersion was prepared employing phosphate ester having short hydrophilic segment as dopant, with electrical conductivity of casting film reached 25 S/cm. Lamellar self-assembly structure was obtained with alternating polyaniline and phosphate ester side chain layers. The side chain crystalline structure showed the periodicity of ca. 1.2 nm. The high electrical conductivity was caused by the side chain crystalline forced lamellar structure. The conductivity decreased with the increasing temperature due to the collapse of dopant side chain crystalline. Lamellar structure due to side chain crystalline confinement may be a new way to improve the electrical conductivity of conducting polyaniline.

Acknowledgment

Financial support from the National Science Foundation of China (Grant No. 20225414) was gratefully acknowledged.

References

[1] Anastas PT, Kirchhoff MM. Acc Chem Res 2002;35(9):686–94.
[2] Wei XL, Wang YZ, Long SM, Bobeczko C, Epstein AJ. J Am Chem Soc 1996;118(11):2545–55.
[3] Shimizu S, Saitoh T, Uzawa M, Yano K, Maniyama T, Watanabe K. Synth Met 1997;85(1–3):1337–8.
[4] Chakraborty M, Mukherjee DC, Mandal BM. Langmuir 2000;16(6):2482–8.
[5] (a) Cao Y, Smith P, Heeger AJ. Synth Met 1993;57(1):3514–9;
(b) Nandan B, Hsu JY, Chiba A, Chen HL, Liao CS, Chen SA, et al. Macromolecules 2007;40(3):395–8.
[6] Yue J, Gordon G, Epstein AJ. Polymer 1992;33(20):4410–8.
[7] (a) Geng YH, Sun ZC, Li J, Jing XB, Wang XH, Wang FS. Polymer 1999;40(20):5723–7;
(b) Wang YJ, Wang XH, Li J, Mo ZS, Zhao XJ, Jing XB, et al. Adv Mater 2001;13(20):1582–5;
(c) Wang QG, Liu NJ, Wang XH, Li J, Zhao XJ, Wang FS. Macromolecules 2003;36(15):5760–4;
(d) Wang YJ, Wang XH, Zhao XJ, Li J, Mo ZS, Jing XB, et al. Macromol Rapid Commun 2002;23(2):118–21.
[8] Luo J, Zhang HM, Wang XH, Li J, Wang FS. Macromolecules 2007;40(23):8132–5.
[9] Li J, Fang K, Qiu H, Li SP, Mao WM. Synth Met 2004;142(1–3):107–11.
[10] Cao Y, Smith P, Heeger AJ. Synth Met 1992;48(1):91–7.
[11] Reghu M, Yoon CO, Moses D, Heeger AJ, Cao Y. Phys Rev B 1993;48(24):17685–94.
[12] MacDiarmid AG, Epstein AJ. Synth Met 1994;65(2–3):103–16.
[13] MacDiarmid AG, Epstein AJ. Mater Res Soc Symp Proc 1994;328:133.
[14] Cao Y, Qiu J, Smith P. Synth Met 1995;69(1–3):187–90.
[15] Cao Y, Smith P. Synth Met 1995;69(1–3):191–2.
[16] Cao Y, Smith P, Heeger AJ. U.S. Patent 5,232,631; 1993.
[17] Yu CL, Zhai J, Gao XF, Wan MX, Jiang L, Li TJ, et al. J Phys Chem B 2004;108(15):4586–9.
[18] Yang CY, Smith P, Heeger AJ, Cao Y, Osterholm JE. Polymer 1994;35(6):1142–7.
[19] Zheng WY, Wang RH, Levon K, Rong ZY, Taka T, Pan W. Macromol Chem Phys 1995;196(8):2443–62.
[20] Kulszewicz BI, Zagorska M, Niziol J, Pron A, Luzny W. Synth Met 2000;114(2):125–31.
[21] Dufour B, Rannou P, Fedorko P, Djurado D, Travers JP, Pron A. Chem Mater 2001;13(11):4032–40.
[22] Olinga TE, Fraysse J, Travers JP, Dufresne A, Pron A. Macromolecules 2000;33(6):2107–13.
[23] Tiitu M, Volk N, Torkkeli M, Serimaa R, Brinke GT, Ikkala O. Macromolecules 2004;37(19):7364–70.
[24] Nandan B, Chen HL, Liao CS, Chen SA. Macromolecules 2004;37(25):9561–70.
[25] Macdiarmid AG, Chiang JC, Richter AF, Epstein AJ. Synth Met 1987;18(1):285–90.
[26] Wang P, Tan KL, Kang ET, Neoh KG. Appl Surf Sci 2002;193(1–4):36–45.
[27] Nabid MR, Sedghi R, Jamaat PR, Safari N, Entezami AA. J Appl Polym Sci 2006;102(3):2929–34.
[28] (a) Masdarolomoor F, Innis PC, Ashraf S, Kaner RB, Wallace GG. Macromol Rapid Commun 2006;27(23):1995–2000;
(b) MacDiarmid AG, Epstein AJ. Synth Met 1995;69:85–92.
[29] Chen SA, Lee HT. Macromolecules 1995;28(8):2858–66.
[30] Xia Y, Wiesinger JM, MacDiarmid AG, Epstein AJ. Chem Mater 1995;7(3):443–5.
[31] (a) Kang ET, Neoh KG, Tan KL. Adv Polym Sci 1993;106:135;
(b) Kang ET, Neoh KG, Tan KL. Prog Polym Sci 1998;23(2):277–324.
[32] Yuet J, Epstein AJ. Macromolecules 1991;24(15):4441–5.
[33] Chen SA, Hwang GW. J Am Chem Soc 1995;117(40):10055–62.
[34] Pouget JP, Jozefowicz M, Epstein AJ, Tang X, MacDiarmid AG. Macromolecules 1991;24(3):779–89.
[35] Fischer JE, Zhu Q, Tang X, Scherr EM, MacDiarmid AG, Cajipe VB. Macromolecules 1994;27(18):5094–101.
[36] Zheng W, Angelopoulos M, Epstein AJ, MacDiarmid AG. Macromolecules 1997;30(24):7634–7.
[37] Moon YB, Cao Y, Smith P, Heeger AJ. Polym Commun 1989;30:196–9.
[38] Han DX, Chu Y, Yang LK, Liu Y, Lu ZX. Colloids Surf A Physicochem Eng Aspects 2005;259(1–3):179–87.
[39] Belosludov RV, Sato H, Farajian AA, Mizuseki H, Kawzeoe Y. Thin Solid Films 2003;438–439:80.
[40] Vilkman M, Kosonen H, Nykänen A, Ruokolainen J, Torkkeli M, Serimaa R, et al. Macromolecules 2005;38(18):7793–7.